MOKE Magnetometer Studies of Evaporated Ni and Ni/Cu Thin Films onto Different Substrates

L. Kerkache, A. Layadi, M. Hemmous, A. Guittoum, M. Mebarki, Nicolas Tiercelin, A. Klimov, Vladimir Preobrazhensky, Philippe Pernod

MOKE magnetometer studies of evaporated Ni and Ni/Cu thin films onto different substrates

L. Kerkache [(1)], A. Layadi [(1)*], M. Hemmous [(2)], A. Guittoum [(2)], M. Mebarki [(3)], N. Tiercelin [(4)], A. Klimov [(4)], V. Preobrazhensky [(4)] and P. Pernod [(4)]

(1) L.E.S.I.M.S., Département de Physique, Université de Sétif 1, Sétif 19000, Algeria

(2) Nuclear Research Centre of Algiers, 2 Bd Frantz Fanon, BP 399, Alger-Gare, Algiers, Algeria

(3) Centre de Recherche en Technologie des Semi-conducteurs pour l'Energétique (CRTSE), 2, Bd Frantz Fanon, BP 140 Alger 7- Merveilles 16038, Algeria

(4) Univ. Lille, CNRS, Centrale Lille, ISEN, Univ. Valenciennes, UMR 8520 IEMN, LIA LICS/LEMAC, F-59000 Lille, France

*Corresponding author: alayadi@univ-setif.dz or A_Layadi@yahoo.fr (A. Layadi)

Abstract

The Magneto-Optic Kerr Effect (MOKE) technique has been used to investigate the magnetic properties of Ni thin films, with thickness t ranging from 9 to 163 nm, evaporated onto several substrates (glass, Si (111), mica and Cu) with and without an evaporated Cu underlayer. The MOKE observations were correlated with the surface morphology inferred from Scanning Electron Microscope images and with the structural properties (grain size and strain). Some interesting behaviors of the coercive field (with values in the 2 to 151 Oe range), the squareness (between 0.1 and 0.91) and the saturation field (25 to 320 Oe) are observed as a function of t, the substrate and the Cu underlayer. A thickness dependent stress-induced anisotropy is found in these films. The differences between the present MOKE results and the ones obtained from the Vibrating Sample magnetometer (VSM) are highlighted. The former describe the surface magnetism of these systems, while the latter are attributed to the whole volume of the sample.

Keywords: Ni films, Ni/Cu films, Evaporation, MOKE, SEM

1. Introduction

A lot of important phenomena are observed in ferromagnetic thin films and multilayers, including Ni films and Ni based multilayers; theses features are interesting for both fundamental research and technological applications [1-5]. The physical properties of thin films strongly depend on the method and the conditions of deposition, on the substrate, and the film thickness. Several works have been reported on Ni films [6-12] and on the Ni/Cu/substrates bilayers [13, 14]. Among the effect of Ni thickness on the physical properties, one may cite (i) the transition from an out-of plane to an in-plane magnetization easy axis, (ii) the effect of the lattice strain on the magnetic moment reduction and (iii) the change from a fine grain structure to a column structure [15-18].

We have used the thermal evaporation to grow series of Ni thin films in the 9 to 163 nm thickness range, deposited on several substrates (glass, Si (111), mica and Cu) with and without an evaporated Cu underlayer. The structural properties of these systems have been published elsewhere [19].Also, we have studied some magnetic properties of these systems as inferred from a Vibrating Sample Magnetometer (VSM) set-up [20].

In the present work, we used the Magneto-Optic Kerr Effect (MOKE) technique to investigate the magnetic properties as a function of the substrates, the Ni thickness and a Cu underlayer. The MOKE technique has been used for a long time as a means for the magnetic characterization of materials [20-22]. The magneto-optical (MO) properties of Ni have been studied by MOKE measurements [23, 24]. Here, in our investigation, we focused on the effect of the substrates, the Ni thickness and the Cu underlayer on the magnetic properties of Ni thin films, such as the coercive and saturation fields, the squarness and the magnetic anisotropy of Ni/substrates films and Ni/Cu/substrates bilayer films. Also, we attempted to correlate the structural and the magnetic properties of Ni and Ni/Cu films, through results from Scanning Electron Microscopy (SEM) and X-ray diffraction experiments. The

deposition conditions and the characterization techniques are shown in section 2. In section 3, we show the results pertaining to the magneto-optical (MOKE) hysteresis curves along with the SEM images. We discuss the effect of thickness, grain size, Cu underlayer and substrates on the magnetic parameters of the hysteresis curves. A summary and a conclusion are given in section 4.

2. Experimental details

The Ni thin films were deposited onto glass, Si (111), mica and Cu substrates using thermal evaporation method from a 99.995 % purified Ni powder. For the Ni/substrates, the pressure was approximately 7.69 x 10^{-7} mbar before evaporation; it rises to 2.86 x 10^{-6} mbar during the evaporation. For the Ni/Cu/substrates, the same purity for the powder (Cu) was used to evaporate the Cu underlayer. The pressure ranges from 1.52 x 10^{-6} and 1.72 x 10^{-6} mbar before evaporation to 1.58 x 10^{-5} and 1.74 x 10^{-5} mbar during the evaporation for the deposition of the Ni and Cu films respectively. The Ni thickness t ranges from 9 to 163 nm and 8 to 67 nm for the Ni/substrates and Ni/Cu/substrates systems, respectively. For the Ni/Cu/substrates system, the Cu underlayer has two thicknesses, 90 nm (with t = 24 nm) and 52 nm (t = 8, 14 and 67 nm). Details on the preparation conditions and on the structural properties of these systems have been reported elsewhere [19]. The surface morphology is studied by means of a Scanning Electron Microscope (SEM). The magneto optical Kerr effect (MOKE) technique has been used to describe the magnetic properties of these samples. Kerr effect experiments were done to get the hysteresis curves, Kerr rotation θ_K vs applied field H. The measurements were done, at room temperature, in the longitudinal configuration with a magnetic field H varying from - 0.5 to 0.5 kOe.

3. Results and discussion

In Fig. 1, we show examples of the magneto-optic Kerr effect (MOKE) hysteresis loops, for the same Ni thickness (t = 50 nm) and different substrates (glass, Si, mica and Cu) (Fig. 1a). In Fig. 1b, we display the curves pertaining to the Ni/Cu/substrate system with t = 24 nm and t_{Cu}= 90 nm. Fig.1a is meant to show the effect of the substrate while by comparing Fig.1b and Fig.1a, we observe the effect of the Cu underlayer.

The effect of the substrate on the hysteresis curves can be clearly seen by comparing the four figures in Fig. 1a. One can see the differences in the curve shapes, the curve area and the different parameters. For the shape for instance, the Ni/glass curve is square while that of the Ni/Cu curve is a more hard-axis like one, this is due to a change in magnetic anisotropy as will be discussed later on. For the area, Ni/glass has the smallest area compared to the other curves; the area under the hysteresis curve is generally related to the energy needed for the motion of the Bloch walls and the reorientation of the magnetic moments of the domains [25]. The magnetic parameters characterizing the curves such as the coercive field, the squarness and the saturation field are also different for each case; theses values have been measured for all samples and will be discussed in the following. One can also see the difference in the curves with the Cu underlayer. Moreover, one should distinguish between the Cu as a substrate which is a bulk material and the Cu underlayer which is an evaporated thin film on top of the substrate; we will see that the effect on the Ni properties is quite different.

Furthermore, Kerr Effet being very sensitive to the film surface state, we are showing in Fig. 2, examples of SEM surface images of some samples along with the hysteresis loops of theses same samples. One can easily note that there are modifications in both the film surface and the corresponding hysteresis curve; for instance, when the surface is uniform as in Fig. 2.a, a square shaped curve is observed and for a less uniform surface, a change of the curve shape is seen, the curves become broader (see Fig.2 b and c). Thus, we believe that at

least, part of the differences in the shape of the hysteresis curves may be due to the effect of the surface morphology and the surface roughness of Ni films.

In the following we will discuss the coercive field, H_C, the squarness S and the saturation field H_S**.** Recall that for each thickness, the four samples were prepared in the same run, i.e. under the same conditions. Thus, for a given thickness, any changes in the magnetic properties of the Ni thin film are due to the effect of the substrate in the Ni/substrate system and to that of the substrate and the Cu underlayer for the Ni/Cu/substrate system. As a general remark, we note that there are broad ranges of values for H_C, S and H_S, depending on the substrate, the Ni thickness and the Cu underlayer. Indeed, H_C values vary from 2 to 151 Oe, the S values can be as low as 0.1 and as high as 0.91 and the saturation field values are found in the 25 to 320 Oe range. Beyond the interesting physics concerning the origins of the values and the behaviors of these magnetic parameters, these broad ranges of values can be quite useful for technological applications, such as in magnetic and magneto-optical recordings; as these large sets of values may allow one to tune the value of one of these magnetic parameters to the required one for a given application by choosing the substrate, varying the thickness or adding or not a Cu underlayer.

In Fig. 3, we show the variation of the coercive field, H_C, as a function of the Ni thickness, t. For the Ni/substrates system (Fig. 3.a), Ni/glass and Ni/Si series have the same behavior: the coercive field monotonically increases with increasing thickness, from about 2 to 54 Oe; for the Ni/glass samples, there is almost a linear increase. On the other hand, the H_C vs t curves for Ni/mica and Ni/Cu go through a minimum at t = 50 nm; the H_C values at this minimum are equal to 32 Oe and 19 Oe for the films deposited on mica and Cu substrates, respectively. The Ni/glass samples are characterized by the lowest H_C values for

all thicknesses. For the thickest film (167 nm), the H_C values are the same for Ni on glass, Si and Cu, and slightly higher for Ni on mica.

For the effect of Cu underlayer, i.e., the Ni/Cu/substrates system, see Fig. 3.b. We note that in the Ni/Cu/mica series, there is a linear increase of the coercive field with increasing Ni thickness. While for the other substrates, we observe a minimum value at t = 24 nm; it should be noted that this particular sample has a Cu thickness equal to 90 nm, different from the other bilayers where the Cu thickness is 52 nm. Thus, this low value might be due to the relatively higher Cu underlayer thickness; a similar behavior was observed by C. A. F. Vaz et al. [26], where they found that H_C decreases with increasing Cu thickness. Note also that for the smallest thickness (08 nm), the bilayers (Ni/Cu) deposited on glass, Si (111) and mica have almost the same coercive field value (2 Oe), i.e. the coercive field is independent of the substrate; also for this thinner film and at least for Ni/Cu/glass and Ni/Cu/Si, the coercive field remains low and the same (2 Oe) as the ones measured in Ni/glass and Ni/Si, i.e, for the thinner film, H_C is low, independent of the substrate and is not affected by the Cu underlayer . On the other hand, for the thickest sample (t = 67 nm), Ni/Cu/Si is characterized by a much higher H_C value (151Oe) compared to the other samples which have closer values (about 70 Oe).

For the sake of comparison with reported Ni thin film H_C values, we can cite few works in this matter. The coercive field values found here for the Ni/substrate system are comparable to those reported in refs. [27] and [28], but are lower than those reported in ref. [29]. The variation of H_C with thickness of the Ni/Cu/Si is similar to the one observed by H. Hwang and al. [30]; also in this same system, the H_C values are similar to those found by G. Gubbiotti and al.[31], but larger than those measured by B. Schirmer and al. [32]. For

comparable thickness, A. Sharma et al. [33] found a coercive field of 130 Oe for Ni (40 nm)/Si sample; this value is higher than the one we found (13 Oe for Ni (42 nm)/Si).

For the origins of the H_C values and behaviors, the following remarks can be made. As for the variation of H_C with t and the fact that H_C is quite high for thicker films, we believe the reason may arise from magnetic anisotropy; we will come back to this point when addressing the magnetic anisotropy later on. To get more insights on the origins of H_C values, we have studied the variation of H_C with the grain size. For the Ni films deposited onto glass and Si (111) substrates, the coercive field H_C values increase with the increase of the average grain size D. In Table 1, we show examples of such a variation of H_C with D. For the Ni/mica, the H_C vs D curve has a minimum, but there is a general increase of H_C with D; while no clear variation of H_C with D is seen for Ni/Cu. For the Ni/Cu/substrate system, beyond a grain size value of about 6 to 8 nm, H_C increases with grain size for all substrates. For Ni/Cu/glass and excluding the sample with the larger Cu thickness (90nm), H_C increases with increasing average grain size. For the low D values and for Ni/Cu/Si (111), we note a monotonous decrease of H_C with D (see Table 1), then an increase for the high D value; no clear variation is noticed for the other substrates in the low D values, but H_C increases for higher D. From this kind of variation of H_C vs D, one may conclude the following. First, one can rule out the pinning of domain walls at the grain boundaries as responsible for the H_C behavior; indeed, if pinning at the grain boundaries were the origin of the coercive field values, H_C would decrease with increasing D. We observe the inverse behavior, thus pinning at the grain boundaries is not the dominant factor in the values of the coercive field in our case. Second, this kind of variation, i.e the increase of H_C with D, was observed in many

materials; for instance, M. Mebarki et al.[34] found this variation in Fe/glass thin film for low D values; this behavior is well described by some models such as in the Hoffmann's theory[35]. Finally as mentioned above about the SEM images, where different magnetic behaviors are correlated with different surface morphologies, the surface state (the rugosity, the size, shape and distribution of the grains) may play an important role in the high values of H_C measured in some samples, it may lead to a lot of pinning sites [29] which constitute a barrier for the motion of the magnetic domain walls, increasing thus the coercive field. Therefore, in our study, we believe that the main origins of the coercive field behavior are the magnetic anisotropy, the grain size effect and the surface morphology which depend on the substrate, the Ni thickness and the Cu underlayer.

The squarness S is defined as the ratio of the remnant Kerr rotation θ_{KR} to the saturation Kerr rotation θ_{KS}, i.e. $S = \theta_{KR}/\theta_{KS}$. In general, the squareness gives information on the remnant state of a magnetic material which is important in fundamental research and also useful in technological applications. The squareness value may be associated to the mechanisms of the magnetization reversal. A small S value may indicate a magnetization rotation; on the other hand, high S values may be associated with domain wall nucleation and motion [33, 36, 37].

For to the Ni/substrates system, the squarness values are shown in Fig.4.a. We found a whole range of S values, from as low as 0.1 to as high as 0.91. The highest S values are observed for a Ni thickness of about 42 to 50 nm in Ni/glass (0.91), Ni/Si (0.91), Ni/mica (0.89) and Ni/Cu (0.87). Note for comparison that for polycrystalline bulk Ni material, S is equal to 0.866 [38]. In the low thickness range, we note an increase of S for Ni/glass and Ni/Si when t increases from 9 nm to 42 nm (for Si) and to 50nm (glass). Beyond this thickness (50 nm), a monotonous decrease of S is seen for all substrates. For the thickest film, the highest squareness is noted in the Ni/mica sample (S = 0.67), while the lowest S value (S

= 0.45) is observed in Ni/Cu and Ni/Si. The latter one (S = 0.45) is comparable to that found by K. Zhang and al. [38] for Ni/Si films. A. Sharma et al. [33] found a value of S equal to 0.82 for Ni (40 nm)/Si; this value is slightly lower than the one we found (S = 0.91) for Ni(42 nm)/Si.

For the Ni/Cu/substrate system, see Fig. 4. b. For the thinner film (8-9 nm), we note that the Cu underlayer induced a decrease of S for the Ni/glass sample but did not affect the S value of the Ni/Si one, even though these two samples were prepared in the same run, compare Fig. 4a and 4b; the decrease in Ni/Cu/glass is quite large (from 0.72 for Ni/glass to 0.1 for Ni/Cu/glass). The variation of S with the Ni thickness does depend on the substrate. For Ni/Cu/glass, S increases in a monotonous manner with t from 0.1 at t = 9 nm to 0.77 at t = 67 nm. The opposite is seen for Ni/Cu/Cu where S gradually decreases with increasing thickness. For the other substrates (Si and mica), S increases with t up to t = 24 nm (and t_{Cu} = 90nm), then slightly decreases when t is increased further. For the largest thickness (t = 67 nm), S is about the same for Ni/Cu on Si, mica and Cu and slightly higher for Ni/Cu on glass.

We also looked at the variation of S with grain size D. For the Ni/substrate system, in the low D values, S increases with increasing D up to D = 5.5 ± 0.2 nm and then drops for higher D values, see Table 1 for Ni/glass and Ni/Si; this is true also for Ni/Cu but not for Ni/mica, where S decreases with D. For the Ni/Cu/substrates system, a monotonous increase of S with D is seen in Ni/Cu/glass. The opposite occurs for Ni/Cu/Cu where S decreases with increasing D. While no clear variation is seen for the Si and mica substrates.

For the Ni/substrate system, the variation of the saturation field H_S with Ni film thickness t is shown in Fig. 5a. We can see that regardless of the substrate, the saturation magnetic field monotonously increases with increasing thickness t. The saturation field values for Ni/Cu thin films are the largest for all thicknesses, while those corresponding to the Ni/mica are the lowest. For comparison with other work in the same conditions, we may cite

that A. Sharma et al.[33] found a saturation field of 230 Oe for Ni (40 nm)/Si; this value is higher than our result (98 Oe) for Ni(42 nm)/Si.

For the Ni/Cu/substrate system, the saturation field vs Ni thickness is shown in Fig. 5b. Here also, we observe an overall increase of H_S with thickness for all substrates; the Cu underlayer did not affect this H_S behavior with t. However, there is a monotonous increase (an almost linear increase with t) for Ni/Cu on Cu and mica substrates, while for Ni/Cu on glass and Si substrates; there is a thickness range (14 to 24 nm) where H_S seems to remain constant before increasing again. For the thinner samples (8 nm), Ni/Cu deposited on glass, Si and mica have the same H_S values. For the thicker samples (67 nm), the H_S values for Ni/Cu on Si, mica and Cu substrates are the same and the value corresponding to Ni/Cu/glass is somewhat higher. We can see that the saturation field strongly depends on the substrates, the Ni thickness and the Cu underlayer. We have also studied the variation of the saturation field H_S with grain size D. For the Ni/glass, Ni/Si and Ni/mica samples, we observe a monotonous increase of H_S with D, see Table 1 for Ni/glass and Ni/Si, as examples. On the other hand, for Ni films deposited on Cu substrate, H_S has a monotonous decrease with increasing D. For the effect of Cu underlayer, we observed an overall increase in the saturation field with the increase of D for the Ni/Cu/glass (see Table 1) and Ni/Cu/Cu. However, for Ni/Cu on Si and mica, we observed a decrease of H_S with D in the low D values (up to D = 7 nm) then H_S increases with D as D is further increased.

It is worth noting that the saturation field values are generally associated with the magnetic anisotropy. For a given direction, a low (high) saturation field value may indicate that this direction is an easy (hard) direction for the magnetization. In our case, the saturation field values are much lower in the thinner films than in the thicker ones (see Fig. 5). We may

infer that a magnetic anisotropy exists; it is strong in thinner films and diminishes as the film thickness increases; it makes the plane direction a much easier one in thinner films than in thicker ones. We conclude this from the H_S behavior and also from the shape of the hysteresis curves; the thinner films curves are characterized by a square, easy direction-like curves with low H_S and H_C, while as the Ni thickness increases, the hysteresis curves become more and more hard direction-like curves with high H_S and H_C values. In order to investigate the origin of this magnetic anisotropy, we made a correlation between the structural and magnetic properties. In these samples, we found that the strain ε values in thinner films are relatively higher than those measured for thicker ones; thinner films are subjected to a higher stress, as the thickness increases, the stress decreases, i.e. the stress is relieved. Thus higher stress values are associated with lower saturation field values; see Table 1, compare the magnitude of the strain and the H_S values for Ni/glass and Ni/Si, with and without Cu underlayer. We may conclude from this correlation between ε and H_S that the origin of the magnetic anisotropy is the stress. Thus, a stress-induced magnetic anisotropy is present in these Ni films; it is stronger in thinner films than in thicker ones. It is detected for Ni on all substrates; however the magnitude of this anisotropy is different from one substrate to the other. In fact magneto-elastic effects have been reported to exist in Ni films under some conditions [39].

Finally, it is interesting to compare the present results obtained by the MOKE technique with the ones measured on these systems by means of the Vibrating Sample Magnetometer (VSM) method [20]. We noticed, indeed that the characteristics of the MOKE hystersis curves are different from the VSM ones. This is expected; the effect was seen in several ferromagnetic materials and was reported by a lot of researchers [40]. One of the main reasons for the differences is the fact that the MOKE technique, based on the interaction of light with the sample, concerns only the surface or a small region near the surface (the

penetration depth of the light); thus the parameters derived from the MOKE method describe the surface magnetism of the sample. On the other hand, the parameters obtained from VSM are average values over the whole volume of the sample. In our case, we can cite few of the main differences between the results. (i) Starting from the last point we discussed, i.e. the saturation field H_S values and the magnetic anisotropy, we found that the H_S values measured from VSM are between 280 Oe and 2400 Oe for the Ni/substrate system and from 520 to about 3200 Oe for the Ni/Cu/substrate; these values are much higher than the H_S values we derived here from MOKE which range from 25 to a maximum of 320 Oe for both systems. It follows that the strength of the magnetic anisotropy over the entire sample volume is more important than that acting on the magnetization on the surface of the sample. (ii) Moreover, for the saturation field and magnetic anisotropy, with the MOKE investigation, we found that there is an overall increase of the H_S values as t increases, for all substrates and for both systems (compare the H_S values at t = 8 nm and t = 163 nm in Fig. 5a and the values at t = 9 nm and t = 67 nm in Fig. 5b). When using the VSM, we noticed that again the monotonous increase of H_S with t is seen in the Ni/substrates for all substrates. However for the Ni/Cu/substrate, the increase of H_S with t is followed for the glass and mica substrates, but for Ni/Cu/Si and Ni/Cu/Cu, we see the opposite, H_S decreases with increasing t. This means that not only the magnitude of the magnetic anisotropy is different in the volume (VSM) and in the surface (MOKE) but also the easy axes in both cases are different. For the MOKE technique, the fact that H_S increases for the thicker films means that the plane becomes a relatively harder direction compared to the thinner films and this applies for all substrates. On the other hand, from VSM, the decrease of H_S for the thicker films, for the Si and mica substrates, means that the plane in these films is becoming a relatively easier direction for the magnetization. Thus once again, the volume of the sample may consist of regions (including

the surface) with different anisotropies; the VSM gives an average value and a resultant easy axis for the whole volume, while with MOKE we may determine the easy axis and the strength of the anisotropy for the surface. (iii) The coercive field values derived from MOKE are lower than those obtained from the VSM for most samples, see Table 2 for some samples given as examples. This is somewhat logical, since as pointed before, part of the H_C values may arise from magnetic anisotropy and we noted that the anisotropy in the volume is different from that at the surface. (iv) Finally, we measured different squareness values (see Table 2) from the two techniques. In most samples, the S values from VSM are lower than the ones from MOKE. Depending on the interest of a researcher, one or the other method may be appropriate. For researchers interested in magneto-optical applications or surface effects, the present MOKE results might be useful and meaningful.

4. Conclusion

The Magneto-Optic Kerr Effect (MOKE) technique is used to probe the surface magnetism of a series of Ni thin films, with thickness t in the nanometer range, evaporated onto glass, Si (111), mica and Cu substrates, and also a second series with a Cu underlayer and the same substrates, i.e Ni/Cu/substrates. We found that the values and the behaviors of the coercive field H_C, the squareness S and the saturation field H_S strongly depend on the substrate, the Ni thickness and the Cu underlayer. For the Ni/glass and Ni/Si series, H_C monotonically increases with increasing t; while for Ni/mica and Ni/Cu, the H_C vs t curves go through a minimum value at t = 50 nm. The Ni/glass samples are characterized by the lowest H_C values. We believe that the main origins of the H_C values and behaviors are the magnetic anisotropy, the grain size effect and the surface morphology. For the latter, different magnetic behaviors are correlated with different surface morphologies as inferred from SEM images. The highest S values (0.87 - 0.91) are observed for t around 50 nm. For the thinnest

film (8-9 nm), Cu underlayer induced a large decrease of S for the Ni/glass sample (from 0.72 for Ni/glass to 0.1 for Ni/Cu/glass), but did not affect the S value of the Ni/Si one. The saturation field H_S monotonously increases with increasing t, regardless of the substrate; the Cu underlayer did not affect this H_S behavior with t. From the correlation of the H_S and the stress values, we may infer that a stress-induced magnetic anisotropy is present in these Ni films; it is stronger in thinner films than in thicker ones. Finally, we pointed out the differences between the MOKE results discussed here and the ones derived from VSM**.** Such a comparison allows one to distinguish the surface magnetism described by the MOKE from the properties of the whole volume associated with the VSM measurements. Among the differences, we found that the magnetic anisotropy for the volume is more important than that at the surface.

References

[1] P. Grünberg, R. Schreiber, Y. Pang, M. B. Brodsky, and H. Sowers, "Layered Magnetic Structures: Evidence for Antiferromagnetic Coupling of Fe Layers across Cr Interlayers", Phys. Rev. Lett.57, 2442 (1986).

[2] Y. Wang, C. H. de Groot, D. Claudio-Gonzalez, and H. Fangohr, "Magnetoresistance in a lithography defined single constrained domain wall spin-valve", Appl. Phys. Lett.97, 262501 (2010).

[3] H. He, Z. Zhang, B. Ma, and Q. Jin, "[Co/Ni]N-based synthetic antiferromagnet with perpendicular anisotropy and its application in pseudo spin valves" , IEEE Trans. Magn.46, 1327 (2010).

[4] J. A. C. Bland and B. Heinrich. Ultrathin Magnetic structures I: " An Introduction to the Electronic, Magnetic and Structural Properties", Springer, 2005.

[5] A. Layadi, J.O. Artman, R.A. Hoffman, C.L. Jensen, D.A. Saunders and B.O. Hall, "Coupling of Ni and NiFe films through an intervening non-magnetic film", J. Appl. Phys. 67, 9, pp. 4451-4453, (1990).

[6] A. L. Dolgiy, S.V. Redko, I. Komissarov, V.P. Bondarenko, K.I. Yanushkevich, S.L. Prischepa. "Structural and magnetic properties of Ni nanowires grown in mesoporous silicon templates ", Thin Solid Films 543 (2013) 133–137.

[7] Z. B. Guo, W.B. Mi, Q. Zhang, B. Zhang, R.O. Aboljadayel, X.X. Zhang, "Anomalous Hall effect in polycrystalline Ni films", Sol. Sta. Com. 152 (2012) 220–224.

[8] Z. Yang, H. Qiu, B. Hu, G. Zou, " Structural and electrical properties of Ni films sputter-deposited on HCl-doped polyaniline substrates", Vacuum. 99 (2014) 192-195.

[9] C. Nacereddine, A. Layadi, A. Guittoum, S.-M. Cherif, T. Chauveau, D. Billet, J. Ben Youssef, A. Bourzami, M. H. Bourahli. , "Structural, electrical and magnetic properties of evaporated Ni/Cu and Ni/glass thin films", Mater. Sci. Eng. B 136 (2007) 197–202.

[10] S.-M. Chérif, A. Layadi, J. Ben Youssef, C. Nacereddine, Y. Roussigné, "Study of the magnetic anisotropy in Ni/Cu and Ni/glass thin films", Physica B 387 (2007) 281–286.

[11] M. Hemmous, A. Layadi, A. Guittoum, A. Bourzami, A. Benabbas, "Effect of deposition rate and thickness on the structural and electrical properties of evaporated Ni/glass and Ni/Si(100) thin films", Microelectronics. J. 39 (2008) 1545 – 154 9.

[12] 48. B. Ghebouli, A. Layadi and L. Kerkache, "Effect of the substrate on the structural and electrical properties of dc sputtered Ni thin films.", Euro. Phys. J.: AP 3, 35-39, (1998).

[13] R. Naik, M. Ahmad, G. L. Dunifer, C. Kota, A. Poli, Ke Fang, U. Rao and J. S. Payson, "Growth and magnetic studies of epitaxial films of Fe, Co and Ni on Cu(100)/Si(100)", J. Magn. Magn. Mater. 121 (1993) 60-64.

[14] H. J. Hug, B. Stiefel, A. Moser, I. Parashikov, A. Klicznik, D. Lipp, H.-J. Güntherodt, G. Bochi, D. I. Paul, R. C. O'Handley, "Magnetic domain structure in ultrathin Cu/Ni/Cu/Si(001) films (invited)" , J. Appl. Phys.79, 5609 (1996).

[15] J. S. Lee, Y. J. Park, J. H. Song, K. H. Chae, J. Lee, C. N. Whang, K . Jeong, D. H. Kim, S. C. Shin, "Modification of interface magnetic anisotropy by ion irradiation on epitaxial Cu/Ni/Cu(002)/ Si(100) films", Phys. Rev. B 69. 172405 (2004).

[16] J. Lee, G. Lauhoff, M. Tselepi, S. Chope, P. Rosenbusch, J. A. C. Bland, H. A. Dürr, V. D. Laan, J. Ph. Schillé, J. A. D. Matthew, "Evidence for a strain-induced variation of the magnetic moment in epitaxial Cu/Ni/Cu/Si(100) structures", Phys. Rev. B 55. 15103 (1997).

[17] G. Lauhoff, J. Lee, J. A. C. Bland, J. Ph. Schill, G. van der Laan, "Ferromagnetic coupling and anisotropy in epitaxial Cu/Co/Ni/Cu (0 0 1)", J. Magn. Magn. Mater. 177-181 (1998) 1253-1254.

[18] G. B. Cho, K. K. Cho, K. W. Kim, "Effects of Ni film thickness on the structural stability of Si/Ni/Cu film electrodes", Mater. Lett. 60 (2006) 90 – 93.

[19] M. Hemmous, A. Layadi, A. Guittoum, N. Souami, M. Mebarki and N. Menni. "Structure, surface morphology and electrical properties of evaporated Ni thin films: Effect of substrates, thickness and Cu underlayer", Thin Solid Films 562 (2014) 229–238.

[20] M. Hemmous, A. Layadi, L. Kerkache, N. Tiercelin, V. Preobrazhensky and P. Pernod, “Magnetic properties of evaporated Ni thin films: Effect of substrates, thickness and Cu underlayer ”, Metallurgical and Materials Transactions A, Vol. 46, issue 9 (2015), 4143-4149.

[20] C. C. Robinson, "Longitudinal Kerr Magneto-Optic Effect in Thin Films of Iron, Nickel, and Permalloy", J. Opt. Soc. Am.53, 681 (1963).

[21] S. Visnovsky, V. Parızek, M. Nyvlt, P. Kielar, V. Prosser, and R. Krishnan, "Magneto-optical Kerr spectra of nickel", J. Magn. Magn. Mater.127, 135 (1993).

[22] A. Hubert and R. Schäfer, "Magnetic Domains: The Analysis of Magnetic Microstructures", Springer-Verlag, Heidelberg, 2000.

[23] J. L. Erskine and E. A. Stern, "Magneto-optic Kerr Effect in Ni, Co, and Fe", Phys. Rev. Lett.30, 1329 (1973).

[24] K. Nakajima, H. Sawada, T. Katayama, and T. Miyazaki, "Effects of the surface and interface on the magneto-optical properties in (Co, Ni)/Cu(001) ultrathin films", Phys. Rev. B54, 15950 (1996).

[25] J. P. Bailon et J. M. Dorlot, "*Des Matériaux"*, Presse Internationale Polytechnique, third edition, Canada, 2000.

[26] C. A. F. Vaz and J. A. C. Bland. "Dependence of the coercive field on the Cu overlayer thickness in thin Co/Cu(001) and Ni/Cu(001) fcc epitaxial films", J. Appl. Phys. 89, 7374 (2001).

[27] S. Z. Wu, G. J. Mankey, F. Huang, R. F. Willis, "Spin reorientation transition in Ni films on Cu(100)", J. Appl. Phys. 76. 6434 (1994).

[28] E. E. Shalyguina, M. A. Mukasheva, N. M. Abrosimova, L. Kozlovskii, E. Tamanis, A. N. Shalygin "The influence of annealing on magnetic and magneto-optical properties of iron and nickel films", J. Magn. Magn. Mater. 300 (2006) e367 – e370.

[29] J. Pflaum, E. Hubner, Th. Zeidler, T. Schmitte, J. Pelzl, "Studies of the influence of the local growth characteristics on the magnetic properties of electrolytically deposited Ni films", Thin Solid Films 318 (1998) 186–188.

[30] H. M. Hwang, J. C. Park, D. G. You, H. S. Park, K. Jeong, and J. Lee, T. G. Kim and J. H. Song, " Spin-reorientation transition of epitaxial Cu/Ni/Cu (001) structure", J. Appl. Phys. 93, 7625 (2003).

[31] G. Gubbiotti, G. Carlotti, F. D'Orazio, F. Lucari, R. Bernardini, M. De Crescenzi, "Magnetic anisotropy in epitaxial Cu/Ni/Cu/Si(1 1 1) ultrathin films studied by magneto-optical Kerr effect and Brillouin spectroscopy", J. Magn. Magn. Mater. 177-181 (1998) 1259-1261.

[32] B. Schirmer and M. Wuttig, "Antiferromagnetic coupling in fcc Fe overlayers on Ni/Cu(100)", Phys. Rev. B 60 (1999) 12945 (5).

[33] A. Sharma, S. Tripathi, K.C. Ugochukwu, J. Tripathi, "Magnetic and structural properties of Ni nanocaps deposited onto self assembled nanosphere array", Thin Solid Films 536 (2013) 249 –255.

[34] M. Mebarki, A. Layadi, L. Kerkache, N. Tiercelin, V. Preobrazhensky, and P. Pernod, “Surface morphology and magnetic properties of evaporated Fe/Si and Fe/glass thin films”, Applied Physics A, Vol. 120, issue 1 (2015) 97-104.

[35] H.S. Jung, W.D. Doyle and S. Matsunuma, "Influence of underlayers on the soft properties of high magnetization FeCo films", J. Appl. Phys. 93, 6462 (2003).

[36] J. Swerts, K. Temst, N. Vandamme, C. Van Haesendonck, Y. Bruynseraede, "Interplay between surface roughness and magnetic properties in Ag/Fe bilayers", J. Magn. Magn. Mater. 240 (2002) 380.

[37] L. Nzoghé-Mendome , A. Aloufy, J. Ebothé, "Nanoscale Topography and Magnetic Structure of Nanocrystallized Nickel Electrodeposits", Mol. Cryst. Liq. Cryst. 555 (2012) 32.

[38] K Zhang, K P Lieb, N Bibic, N Pilet, T V Ashworth, M A Marioni and H J Hug, " Microstructural and magnetic properties of thermally mixed Ni/Si bilayers", J. Phys. D: Appl. Phys. 41 (2008) 095003.

[39] K. Ha, R.C. O’Handley, "Magnetization canting in epitaxial Cu/Ni/Cu/Si(001) films", J. Appl. Phys. 87 (2000) 5944.

[40] A. Hendrych, O. Zivotsky, J. Jiraskova and I. Matko, "The Surface and Bulk Magnetic Properties of Fe-Al Alloys ", Acta physica Polonica A, 126 (2014) 58.

Table and Figure captions

Table. 1. Strain ε **,** average grain size D, coercive field H_C, squareness S and saturation field H_S for Ni thin films evaporated on glass and Si substrates with and without Cu underlayer.

Table. 2. Comparison between the MOKE and the VSM results, for Ni/substrates and Ni/Cu/substrates (substrates as indicated); t : the Ni thickness, H_C : the coercive field, S : the squareness and H_S : the saturation field.

Fig. 1. The longitudinal Kerr hysteresis loops for (a) Ni/glass, Ni/Si, Ni/Cu and Ni/mica with t = 50 nm (effect of the substrat); (b) Ni/Cu/glass, Ni/Cu/Si, Ni/Cu/Cu and Ni/Cu/mica with t = 24 nm and t_{Cu}= 90 nm (effect of the Cu underlayer and susbtrate).

Fig. 2. Examples of SEM surface images and the corresponding hysteresis loops for (a) Ni (42 nm)/Si (111), (b) Ni (14 nm)/Cu (52 nm)/Si (111) and (c) Ni (67 nm)/Cu(52 nm)/Si (111).

Fig. 3. Coercive field H_C vs Ni thickness for (a) Ni films on glass, Si, mica and Cu substrates and (b) Ni/Cu/Substrates with substrates as indicated.

Fig. 4. Squareness S vs Ni thickness for (a) Ni films on glass, Si, mica and Cu substrates and (b) Ni/Cu/Substrates with substrates as indicated.

Fig. 5. Saturation field H_S vs Ni thickness for (a) Ni films on glass, Si, mica and Cu substrates and (b) Ni/Cu/Substrates with substrates as indicated.

Ni/substrates						Ni / Cu/ substrates				
substrate	ε (%)	D (nm)	Hc (Oe)	S	Hs (Oe)	ε (%)	D (nm)	Hc (Oe)	S	Hs (Oe)
glass	0.77	4.4	2	0.72	50	-1.72	5.6	02	0.1	32
	-0.66	4.9	13	0.86	75	-0.66	6.6	57	0.48	115
	-0.22	5.3	15	0.91	100	-0.22	8	10	0.50	110
	-0.34	13.7	54	0.51	130	-0.34	14.1	77	0.77	320
Si (111)	0.55	5	2	0.63	62	-0.77	5.6	41	0.75	85
	0.20	5.5	13	0.91	98	-0.34	6.2	18	0.81	75
	0.02	6.8	26	0.85	112	-1.05	6.6	01	0.60	25
	-0.05	15	55	0.45	162	-0.05	13	151	0.65	220

Table. 1

Table. 1. Strain ε **,** average grain size D, coercive field H_C, squareness S and saturation field H_S for Ni thin films evaporated on glass and Si substrates with and without Cu underlayer.

			MOKE				VSM	
	Substrate	t (nm)	Hc (Oe)	S	Hs (Oe)	Hc (Oe)	S	Hs (Oe)
Ni/substrate	Si	9	2	0.63	62	3.6	0.46	780
	glass	163	54	0.51	130	138	0.26	2250
	Si	163	55	0.45	160	153	0.23	2400
	Mica	163	65	0.67	120	115	0.36	1480
Ni/Cu/Substrate	glass	8	2	0.10	32	5.7	0.22	1500
	glass	67	77	0.77	320	230	0.48	2500
	Cu	67	65	0.63	225	57	0.67	1270
	Mica	67	77	0.64	220	168	0.46	1480

Table. 2

Table. 2. Comparison between the MOKE and the VSM results, for Ni/substrates and Ni/Cu/substrates (substrates as indicated); t : the Ni thickness, H_C : the coercive field, S : the squareness and H_S : the saturation field.

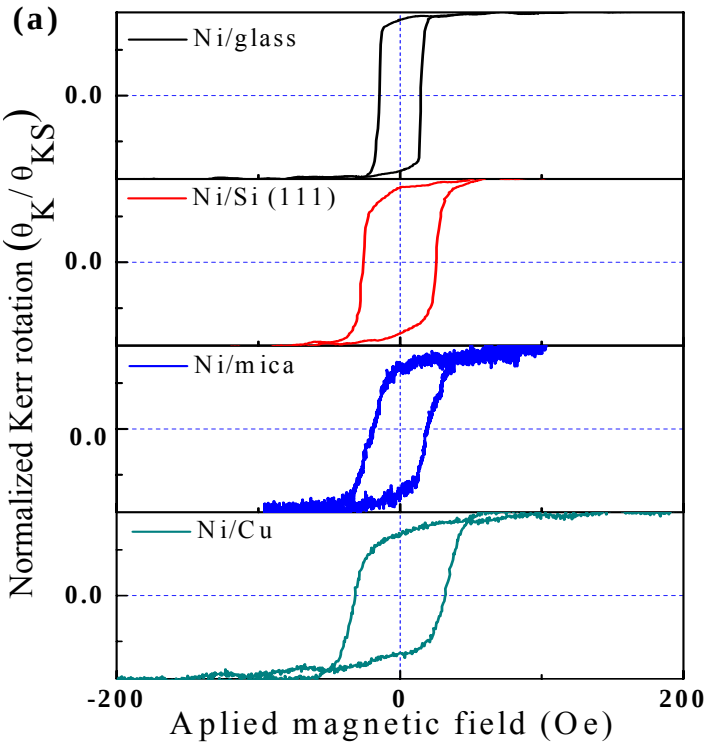
(a)
Ni/glass
Ni/Si (111)
Ni/mica
Ni/Cu
0.0
0.0
0.0
0.0
-200
0
200
Aplied magnetic field (Oe)
Normalized Kerr rotation (θK/θKS)

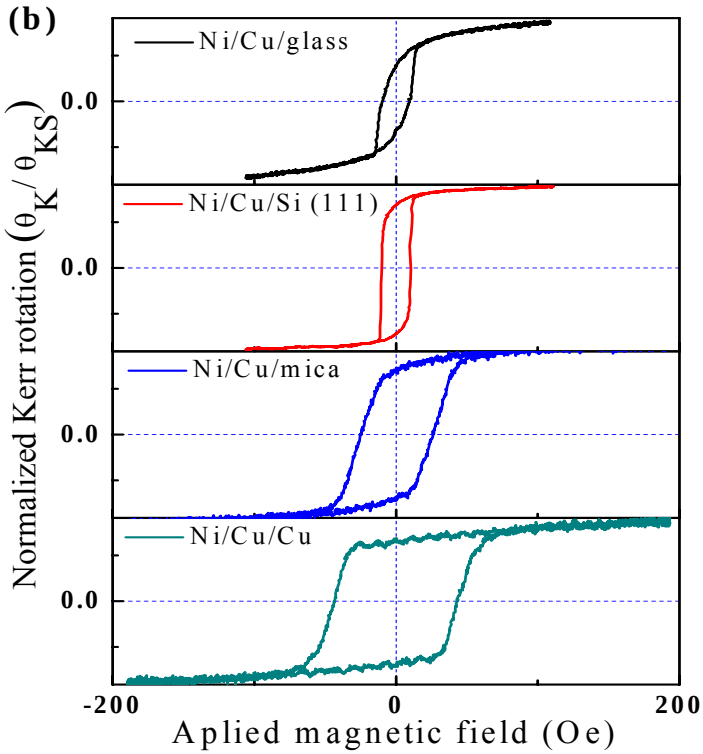
(b)
Ni/Cu/glass
Ni/Cu/Si (111)
Ni/Cu/mica
Ni/Cu/Cu
0.0
0.0
0.0
0.0
-200
0
200
Aplied magnetic field (Oe)
Normalized Kerr rotation (θK/θKS)

Fig. 1. The longitudinal Kerr hysteresis loops for (a) Ni/glass, Ni/Si, Ni/Cu and Ni/mica with t = 50 nm (effect of the substrat); (b) Ni/Cu/glass, Ni/Cu/Si, Ni/Cu/Cu and Ni/Cu/mica with t = 24 nm and t_{Cu}= 90 nm (effect of the Cu underlayer and substrate).

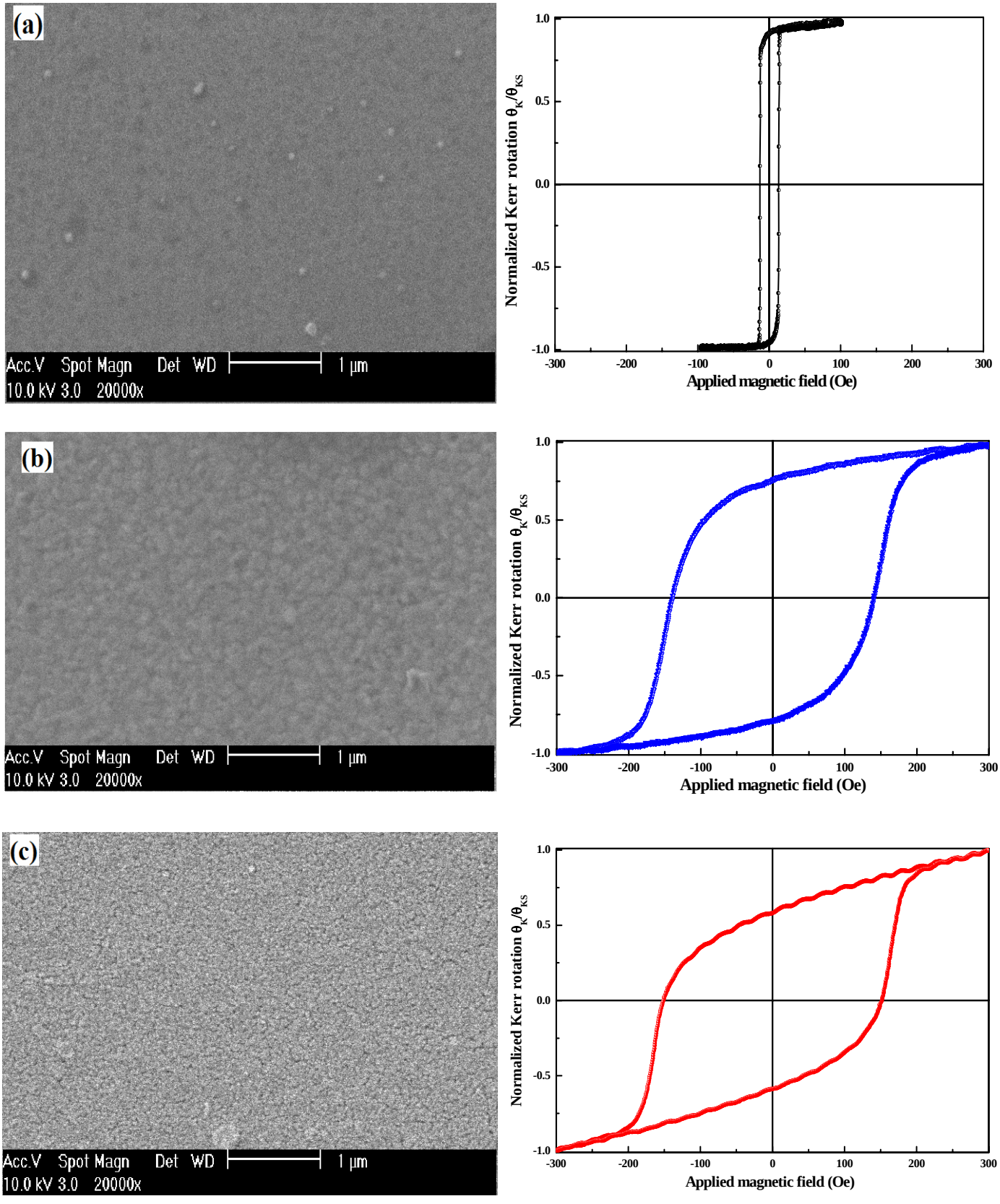

Fig. 2. Examples of SEM surface images and the corresponding hysteresis loops for (a) Ni (42 nm)/Si (111), (b) Ni (14 nm)/Cu (52 nm)/Si (111) and (c) Ni (67 nm)/Cu(52 nm)/Si (111).

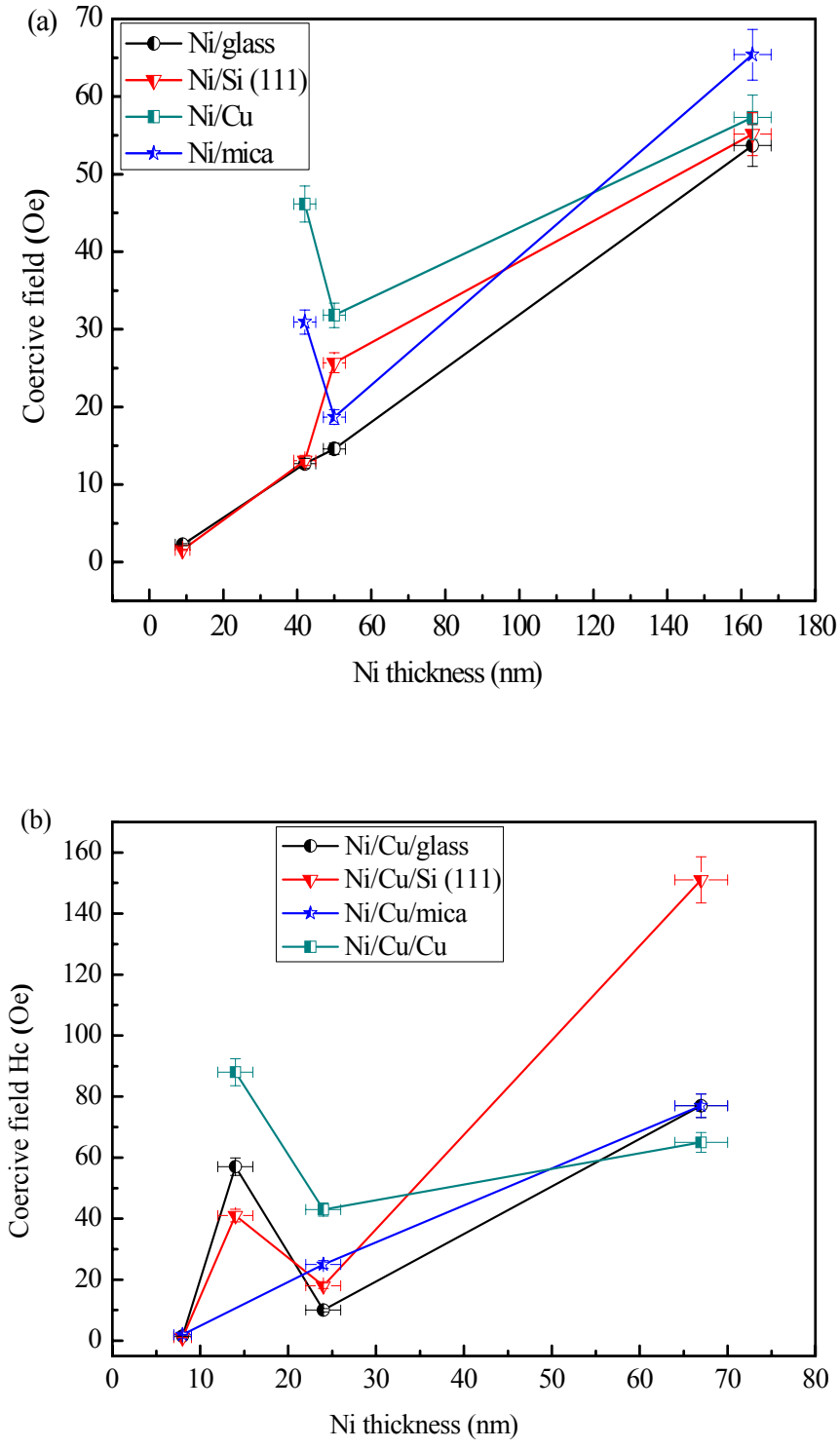

Fig. 3. Coercive field H_C vs Ni thickness for (a) Ni films on glass, Si, mica and Cu substrates and (b) Ni/Cu/Substrates with substrates as indicated.

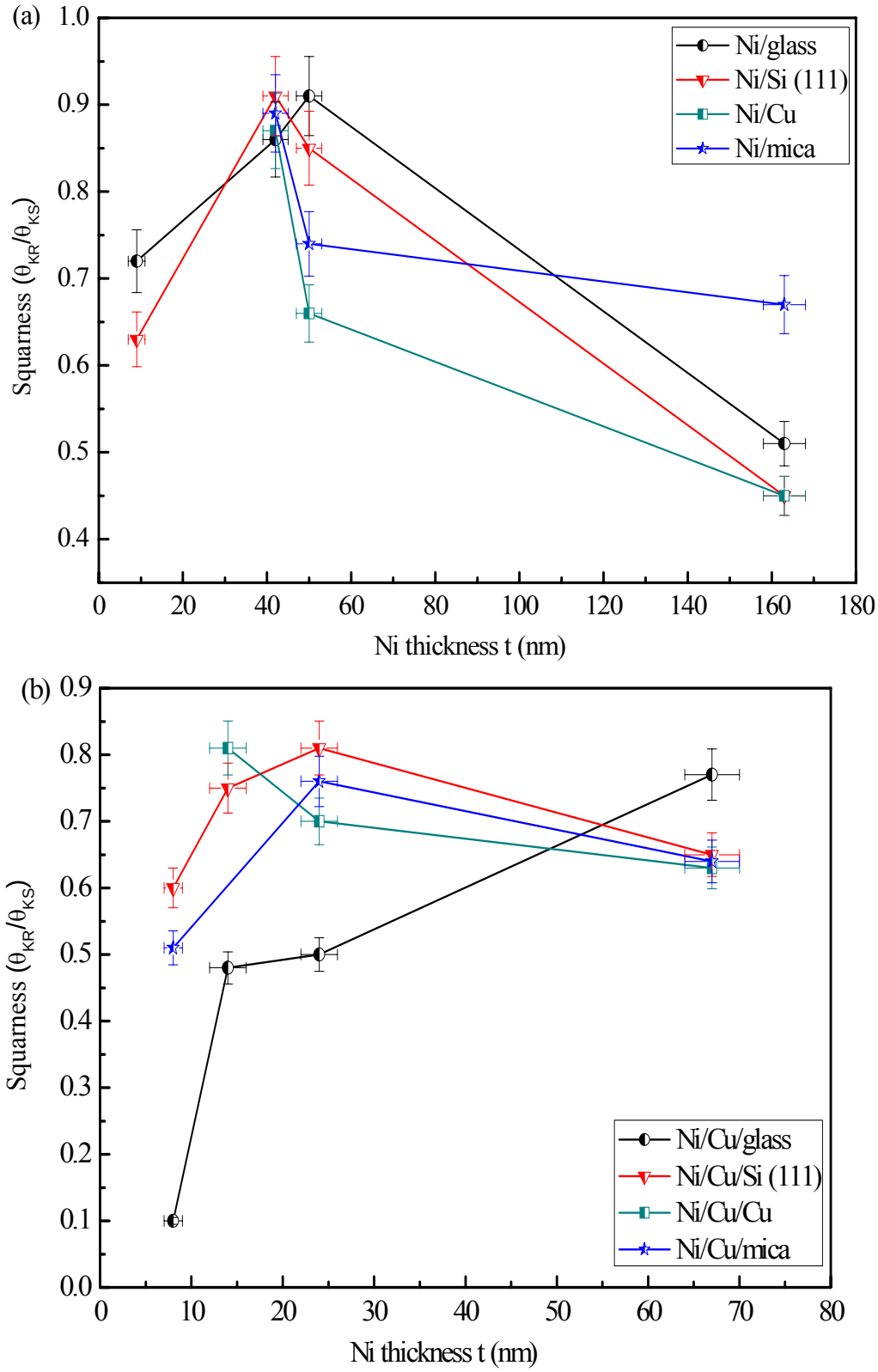

Fig. 4. Squareness S vs Ni thickness for (a) Ni films on glass, Si, mica and Cu substrates and (b) Ni/Cu/Substrates with substrates as indicated.

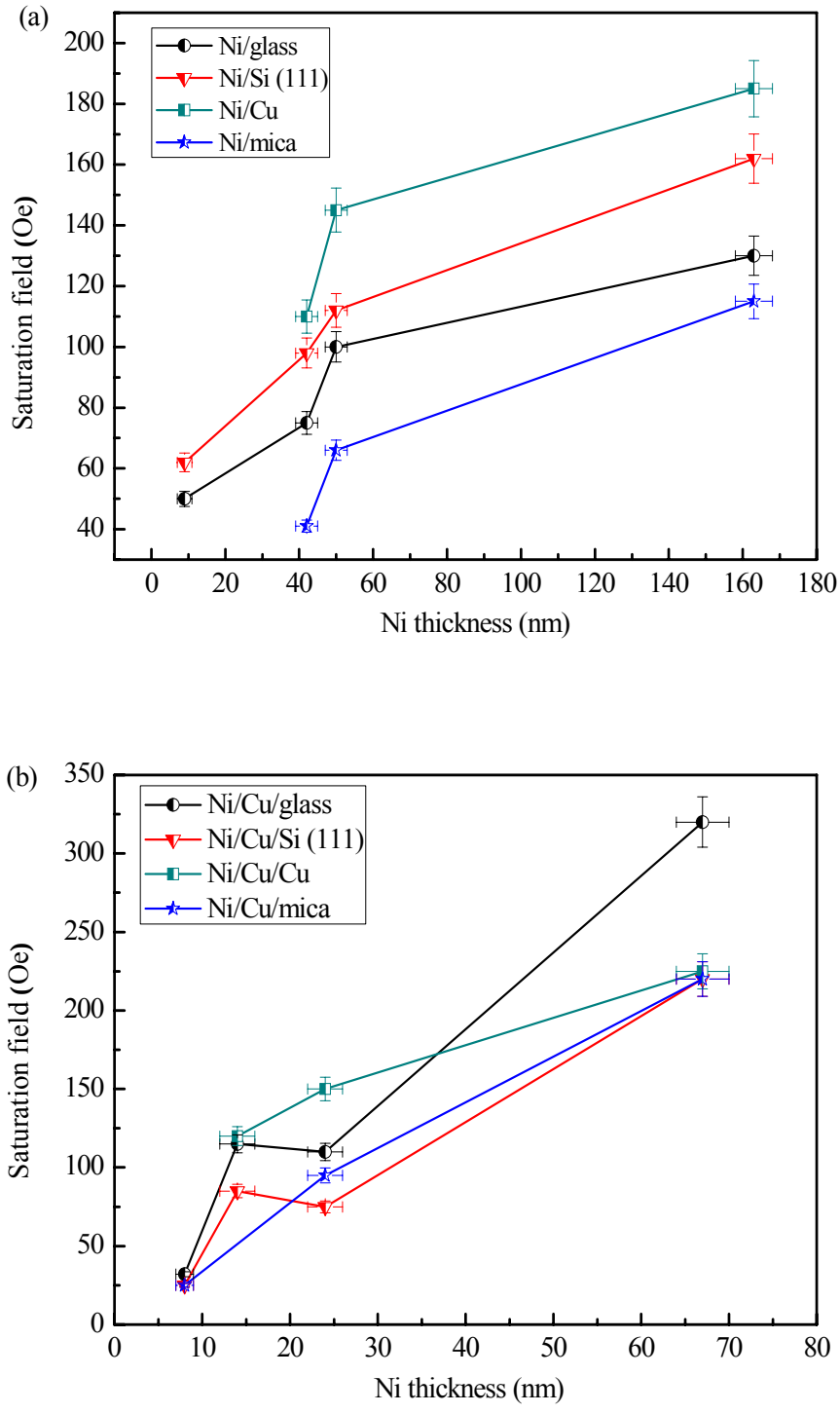

Fig. 5. Saturation field H_S vs Ni thickness for (a) Ni films on glass, Si, mica and Cu substrates and (b) Ni/Cu/Substrates with substrates as indicated.